BIT manuscript No.
(will be inserted by the editor)

Stochastic Runge-Kutta methods with deterministic high order for ordinary differential equations

Yoshio Komori · **Evelyn Buckwar**

Received: date / Accepted: date

Abstract We consider embedding deterministic Runge-Kutta methods with high order into weak order stochastic Runge-Kutta (SRK) methods for non-commutative stochastic differential equations (SDEs). As a result, we have obtained weak second order SRK methods which have good properties with respect to not only practical errors but also mean square stability. In our stability analysis, as well as a scalar test equation with complex-valued parameters, we have used a multi-dimensional non-commutative test SDE. The performance of our new schemes will be shown through comparisons with an efficient and optimal weak second order scheme proposed by Debrabant and Rößler (2009).

Keywords Weak second order · Explicit method · Itô stochastic differential equation · Mean square stability

Mathematics Subject Classification (2000) 65C30 · 60H10 · 60H35

1 Introduction

We are concerned with developing and analyzing weak second order explicit stochastic Runge-Kutta (SRK) methods for non-commutative stochastic differential equations (SDEs). Among such methods, derivative-free methods are especially important

This is a significantly revised work of a proceedings paper in AIP Conference Proceedings 1389, pp. 1590-1593. The work was partially supported by JSPS Grant-in-Aid for Scientific Research No. 23540143.

Yoshio Komori
Department of Systems Design and Informatics, Kyushu Institute of Technology, 680-4 Kawazu, Iizuka, 820-8502, Japan
Tel.: +81-948-7731
Fax: +81-948-7709
E-mail: komori@ces.kyutech.ac.jp

Evelyn Buckwar
Institute for Stochastics, Johannes Kepler University Linz, Altenberger Street 69, A-4040 Linz, Austria
Tel.: +43-732-2468-4161
E-mail: Evelyn.Buckwar@jku.at

because they can numerically solve SDEs with less computational effort compared to other methods which need derivatives.

In fact, weak second order and derivative-free methods have been recently studied by many researchers. Kloeden and Platen [11, pp. 486–487] have proposed a derivative-free numerical scheme of weak order two for non-commutative Itô SDEs. Tocino and Vigo-Aguiar [21] have also proposed it as an example in their SRK family. Komori [12] has proposed a different scheme which is for non-commutative Stratonovich SDEs and which has the advantage that it can reduce the number of random variables that need to be simulated. This scheme, however, still has the drawback that its computational cost for each diffusion coefficient linearly depends on the dimension of the Wiener process. Rößler [16] and Debrabant and Rößler [5] have proposed new schemes which overcome this drawback for Stratonovich and Itô SDEs, respectively, while keeping the advantage mentioned above.

Komori and Burrage [13] have also proposed an efficient SRK scheme which overcomes this drawback by improving the scheme in [12]. In addition, they have indicated that, even in a 10-dimensional Wiener process case, not only the scheme in [13] but also the other one in [12] can perform much better than an efficient scheme [16] in terms of computational costs. The classical Runge-Kutta (RK) method is embedded in both methods [12,13]. This fact motivates us.

In the present paper we consider embedding deterministic high order RK methods into weak second order SRK methods proposed by Rößler [17] for non-commutative Itô SDEs. In stability analysis on numerical methods for SDEs, scalar test SDEs were used very often for about one decade [8,9,14,18], but very recently some researchers have proposed or started to use multi-dimensional test SDEs [2,4,19,20]. Especially, Buckwar and Sickenberger [4] have proposed a two-dimensional test stochastic differential equation (SDE) with non-commutative noise terms expressed by a few parameters, and they have given general results for two methods. We use a more generalized test SDE as well as a scalar test SDE, and utilize their general results.

The paper is organized as follows. In Section 2 we will introduce the SRK methods that we deal with and will solve order conditions for weak order two. In Section 3 we will study mean square stability properties for our new SRK methods. In Section 4 we will investigate their effectiveness in computation by numerical experiments, comparing them with the DRI1 scheme proposed by Debrabant and Rößler [5], which is an efficient weak second order scheme with minimized error constant. Finally, we will give conclusions.

2 SRK methods for weak approximations

Consider the autonomous d-dimensional Itô SDE

$$\mathrm{d}\boldsymbol{y}(t) = \boldsymbol{g}_0(\boldsymbol{y}(t))\mathrm{d}t + \sum_{j=1}^{m} \boldsymbol{g}_j(\boldsymbol{y}(t))\mathrm{d}W_j(t), \quad t > 0, \quad \boldsymbol{y}(0) = \boldsymbol{x}_0, \tag{2.1}$$

where $W_j(t)$ is a scalar Wiener process and $\boldsymbol{x}_0$ is independent of $W_j(t) - W_j(0)$ for $t > 0$. We assume a global Lipschitz condition is satisfied such that the SDE has exactly one continuous global solution on the entire interval $[0,\infty)$ [1, p. 113]. For a given time T_{end}, let t_n be an equidistant grid point nh $(n = 0,1,\ldots,M)$ with step size $h \stackrel{\text{def}}{=} T_{end}/M < 1$ (M is a natural number) and let $\boldsymbol{y}_n$ be a discrete approximation to the solution $\boldsymbol{y}(t_n)$ of (2.1). In addition, let $C_P^L(\boldsymbol{R}^d,\boldsymbol{R})$ be the family of L times continuously differentiable real-valued functions on $\boldsymbol{R}^d$, whose partial derivatives of order less than or equal to L have polynomial growth. Further, suppose that all moments of the initial value $\boldsymbol{x}_0$ exist and $\boldsymbol{g}_j$ $(j = 0,1,\ldots,m)$ are Lipschitz continuous with all their components belonging to $C_P^{2(q+1)}(\boldsymbol{R}^d,\boldsymbol{R})$. Then, the definition of weak convergence of order q is given as follows [11, p. 327].

Definition 2.1 Suppose that discrete approximations $\boldsymbol{y}_n$ are given by a numerical scheme. Then, we say that the scheme is of weak (global) order q if for all $G \in C_P^{2(q+1)}(\boldsymbol{R}^d,\boldsymbol{R})$, constants $C > 0$ (independent of h) and $\delta_0 > 0$ exist, such that

$$|E[G(\boldsymbol{y}(t_M)] - E[G(\boldsymbol{y}_M)]| \leq Ch^q, \quad h \in (0,\delta_0).$$

On the basis of the SRK framework proposed by Rößler [17], we consider the following SRK method for the approximation of Eq. (2.1):

$$\begin{aligned}
\boldsymbol{H}_i^{(0)} &= \boldsymbol{y}_n + \sum_{k=1}^{i-1} A_{ik}^{(0)} h\boldsymbol{g}_0\left(\boldsymbol{H}_k^{(0)}\right) \quad (1 \leq i \leq s-2),\\
\boldsymbol{H}_i^{(0)} &= \boldsymbol{y}_n + \sum_{k=1}^{i-1} A_{ik}^{(0)} h\boldsymbol{g}_0\left(\boldsymbol{H}_k^{(0)}\right) + \sum_{k=s-2}^{i-1}\sum_{l=1}^{m} B_{ik}^{(0)} \triangle\hat{W}_l \boldsymbol{g}_l\left(\boldsymbol{H}_k^{(l)}\right) \quad (i = s-1, s),\\
\boldsymbol{H}_{s-2}^{(j)} &= \boldsymbol{y}_n + \sum_{k=1}^{s-2} A_{s-2,k}^{(1)} h\boldsymbol{g}_0\left(\boldsymbol{H}_k^{(0)}\right) \quad (1 \leq j \leq m),\\
\boldsymbol{H}_i^{(j)} &= \boldsymbol{y}_n + \sum_{k=1}^{i} A_{ik}^{(1)} h\boldsymbol{g}_0\left(\boldsymbol{H}_k^{(0)}\right) + \sum_{k=s-2}^{i-1} B_{ik}^{(1)} \sqrt{h}\boldsymbol{g}_j\left(\boldsymbol{H}_k^{(j)}\right)\\
&\qquad\qquad\qquad\qquad\qquad\qquad (i = s-1, s \text{ and } 1 \leq j \leq m),\\
\hat{\boldsymbol{H}}_i^{(j)} &= \boldsymbol{y}_n + \sum_{k=1}^{s} A_{ik}^{(2)} h\boldsymbol{g}_0\left(\boldsymbol{H}_k^{(0)}\right) + \sum_{k=s-2}^{s}\sum_{\substack{l=1\\ l\neq j}}^{m} B_{ik}^{(2)} \tilde{\eta}^{(j,l)} \boldsymbol{g}_l\left(\boldsymbol{H}_k^{(l)}\right)\\
&\qquad\qquad\qquad\qquad\qquad\qquad (s-2 \leq i \leq s \text{ and } 1 \leq j \leq m),\\
\boldsymbol{y}_{n+1} &= \boldsymbol{y}_n + \sum_{i=1}^{s} \alpha_i h\boldsymbol{g}_0\left(\boldsymbol{H}_i^{(0)}\right) + \sum_{i=s-2}^{s}\sum_{j=1}^{m} \beta_i^{(1)} \triangle\hat{W}_j \boldsymbol{g}_j\left(\boldsymbol{H}_i^{(j)}\right)\\
&\quad + \sum_{i=s-2}^{s}\sum_{j=1}^{m} \beta_i^{(2)} \tilde{\eta}^{(j,j)} \boldsymbol{g}_j\left(\boldsymbol{H}_i^{(j)}\right)\\
&\quad + \sum_{i=s-2}^{s}\sum_{j=1}^{m} \beta_i^{(3)} \triangle\hat{W}_j \boldsymbol{g}_j\left(\hat{\boldsymbol{H}}_i^{(j)}\right) + \sum_{i=s-2}^{s}\sum_{j=1}^{m} \beta_i^{(4)} \sqrt{h}\boldsymbol{g}_j\left(\hat{\boldsymbol{H}}_i^{(j)}\right),
\end{aligned} \tag{2.2}$$

where the α_i, $\beta_i^{(r_a)}$, $A_{ik}^{(r_b)}$, and $B_{ik}^{(r_b)}$ $(1 \leq r_a \leq 4$ and $0 \leq r_b \leq 2)$ denote the parameters of the method. The random variables involved in the scheme are given by $\tilde{\eta}^{(j,j)} \stackrel{\text{def}}{=}$

Table 2.1 Butcher tableau in general form

$A^{(0)}_{21}$										
$\vdots$	$\ddots$									
$A^{(0)}_{s-1,1}$	$\cdots$	$A^{(0)}_{s-1,s-2}$			$B^{(0)}_{s-1,s-2}$					
$A^{(0)}_{s,1}$	$\cdots$	$A^{(0)}_{s,s-2}$	$A^{(0)}_{s,s-1}$		$B^{(0)}_{s,s-2}$	$B^{(0)}_{s,s-1}$				
$A^{(1)}_{s-2,1}$	$\cdots$	$A^{(1)}_{s-2,s-2}$								
$A^{(1)}_{s-1,1}$	$\cdots$	$A^{(1)}_{s-1,s-2}$	$A^{(1)}_{s-1,s-1}$		$B^{(1)}_{s-1,s-2}$					
$A^{(1)}_{s,1}$	$\cdots$	$A^{(1)}_{s,s-2}$	$A^{(1)}_{s,s-1}$	$A^{(1)}_{s,s}$	$B^{(1)}_{s,s-2}$	$B^{(1)}_{s,s-1}$				
$A^{(2)}_{s-2,1}$	$\cdots$	$A^{(2)}_{s-2,s-2}$	$A^{(2)}_{s-2,s-1}$	$A^{(2)}_{s-2,s}$	$B^{(2)}_{s-2,s-2}$	$B^{(2)}_{s-2,s-1}$	$B^{(2)}_{s-2,s}$			
$A^{(2)}_{s-1,1}$	$\cdots$	$A^{(2)}_{s-1,s-2}$	$A^{(2)}_{s-1,s-1}$	$A^{(2)}_{s-1,s}$	$B^{(2)}_{s-1,s-2}$	$B^{(2)}_{s-1,s-1}$	$B^{(2)}_{s-1,s}$			
$A^{(2)}_{s,1}$	$\cdots$	$A^{(2)}_{s,s-2}$	$A^{(2)}_{s,s-1}$	$A^{(2)}_{s,s}$	$B^{(2)}_{s,s-2}$	$B^{(2)}_{s,s-1}$	$B^{(2)}_{s,s}$			
α_1	$\cdots$	α_{s-2}	α_{s-1}	α_s	$\beta^{(1)}_{s-2}$	$\beta^{(1)}_{s-1}$	$\beta^{(1)}_{s}$	$\beta^{(2)}_{s-2}$	$\beta^{(2)}_{s-1}$	$\beta^{(2)}_{s}$
					$\beta^{(3)}_{s-2}$	$\beta^{(3)}_{s-1}$	$\beta^{(3)}_{s}$	$\beta^{(4)}_{s-2}$	$\beta^{(4)}_{s-1}$	$\beta^{(4)}_{s}$

$((\triangle\hat{W}_j)^2-h)/(2\sqrt{h})$,

$$\tilde{\eta}^{(j,l)} \stackrel{\text{def}}{=} \begin{cases} (\triangle\hat{W}_j\triangle\hat{W}_l-\sqrt{h}\triangle\tilde{W}_j)/(2\sqrt{h}) & (j<l), \\ (\triangle\hat{W}_j\triangle\hat{W}_l+\sqrt{h}\triangle\tilde{W}_l)/(2\sqrt{h}) & (j>l), \end{cases}$$

the $\triangle\tilde{W}_l$ $(1\le l\le m-1)$ are independent two-point distributed random variables with $P(\triangle\tilde{W}_j=\pm\sqrt{h})=1/2$ and the $\triangle\hat{W}_j$ $(1\le j\le m)$ are independent three-point distributed random variables with $P(\triangle\hat{W}_j=\pm\sqrt{3h})=1/6$ and $P(\triangle\hat{W}_j=0)=2/3$ [11, p. 225]. Here, (2.2) is characterized by the Butcher tableau in Table 2.1.

In addition to the SRK framework, Rößler [17] has given 59 order conditions for it to achieve weak order two. In order to satisfy the order conditions, we have to suppose $s\ge 3$ when we consider explicit SRK methods. In fact, Debrabant and Rößler [5] have supposed $s=3$ and given the families of the solutions. Let us utilize some of their results because (2.2) has the stochastic parts for $i=s-2,s-1,s$ only. That is, we assume

$$\begin{aligned}
&\beta^{(1)}_{s-2}=\frac{-1+2\left(B^{(1)}_{s-1,s-2}\right)^2}{2\varepsilon_1\left(B^{(1)}_{s-1,s-2}\right)^2}, \quad \beta^{(1)}_{s-1}=\beta^{(1)}_{s}=\frac{1}{4\varepsilon_1\left(B^{(1)}_{s-1,s-2}\right)^2}, \\
&\beta^{(2)}_{s-2}=0, \quad \beta^{(2)}_{s-1}=-\beta^{(2)}_{s}=\frac{1}{2B^{(1)}_{s-1,s-2}}, \quad \beta^{(3)}_{s-2}=-\frac{1}{2\varepsilon_1 b^2_{s-1}}, \\
&\beta^{(3)}_{s-1}=\beta^{(3)}_{s}=\frac{1}{4\varepsilon_1 b^2_{s-1}}, \quad \beta^{(4)}_{s-2}=0, \quad \beta^{(4)}_{s-1}=-\beta^{(4)}_{s}=\frac{1}{2b_{s-1}}
\end{aligned} \tag{2.3}$$

and

$$\begin{aligned} &B^{(0)}_{s,s-1}=0, \quad B^{(1)}_{s,s-2}=-B^{(1)}_{s-1,s-2}, \quad B^{(1)}_{s,s-1}=0,\\ &B^{(2)}_{s-2,s-2}=B^{(2)}_{s-2,s-1}=B^{(2)}_{s-2,s}=0, \quad B^{(2)}_{s-1,s}=B^{(2)}_{s-1,s-1},\\ &B^{(2)}_{s,s-2}=-B^{(2)}_{s-1,s-2}, \quad B^{(2)}_{s,s-1}=B^{(2)}_{s,s}=-B^{(2)}_{s-1,s-1} \end{aligned} \tag{2.4}$$

when $B^{(1)}_{s-1,s-2}$, $B^{(2)}_{s-1,s-2}$ and $B^{(2)}_{s-1,s-1}$ are given. Here, $\varepsilon_1 \stackrel{\text{def}}{=} \pm 1$ and $b_{s-1} \stackrel{\text{def}}{=} B^{(2)}_{s-1,s-2} + 2B^{(2)}_{s-1,s-1}$. Similarly, taking their results into account as well as simplicity, we assume

$$\begin{aligned} &A^{(1)}_{s-1,k}=A^{(1)}_{s,k} \quad (1\le k\le s-2), \quad A^{(1)}_{s-1,s-1}=A^{(1)}_{s,s-1}=A^{(1)}_{s,s}=0,\\ &A^{(2)}_{s-2,k}=A^{(2)}_{s-1,k}=A^{(2)}_{s,k} \quad (1\le k\le s). \end{aligned}$$

In the end, because we embed deterministic high order RK methods into our SRK methods, only the following three order conditions remain to be solved:

$$\begin{aligned} &1.\ \ \sum_{i=s-1}^{s}\alpha_i\left(B^{(0)}_{i,s-2}\right)^2=\frac{1}{2}, \quad 2.\ \ \sum_{i=s-1}^{s}\alpha_i B^{(0)}_{i,s-2}=\frac{\varepsilon_1}{2},\\ &3.\ \ \sum_{i=s-2}^{s}\beta^{(1)}_i\left(\sum_{k=1}^{s-2}A^{(1)}_{ik}\right)=\frac{\varepsilon_1}{2}. \end{aligned}$$

Here, note that each of these corresponds to Conditions 11, 12 and 13 in [5], respectively.

From Conditions 1 and 2, we obtain

$$B^{(0)}_{s-1,s-2}=\frac{(\alpha_{s-1}/\varepsilon_1)\pm\sqrt{\gamma_1}}{2\alpha_{s-1}(\alpha_{s-1}+\alpha_s)}, \qquad B^{(0)}_{s,s-2}=\frac{(\alpha_s/\varepsilon_1)\mp\sqrt{\gamma_1}}{2\alpha_s(\alpha_{s-1}+\alpha_s)} \tag{2.5}$$

(double sign in same order) if $\alpha_{s-1}\neq 0$, $\alpha_s\neq 0$, $\alpha_{s-1}\neq -\alpha_s$ and

$$\gamma_1 \stackrel{\text{def}}{=} \alpha_{s-1}\alpha_s\big(-1+2(\alpha_{s-1}+\alpha_s)\big)\ge 0. \tag{2.6}$$

Taking into account that $B^{(0)}_{s-1,s-2}$, $B^{(0)}_{s,s-2}$, $\beta^{(1)}_i$ and $\beta^{(3)}_i$ $(i=s-2,s-1,s)$ are multiplied by $\triangle\hat{W}_j$ $(1\le j\le m)$ in (2.2), in the sequel we suppose $\varepsilon_1=1$ without loss of generality. Because of our assumption on $A^{(1)}_{ik}$, Condition 3 automatically holds if

$$\sum_{k=1}^{s-2}A^{(1)}_{s-2,k}=\sum_{k=1}^{s-2}A^{(1)}_{s-1,k}=\frac{1}{2}, \tag{2.7}$$

or we have $B^{(1)}_{s-1,s-2}=\pm\sqrt{\gamma_2}$ from Condition 3 if

$$\gamma_2 \stackrel{\text{def}}{=} \left(\sum_{k=1}^{s-2}A^{(1)}_{s-1,k}-\sum_{k=1}^{s-2}A^{(1)}_{s-2,k}\right)\Bigg/\left(1-2\sum_{k=1}^{s-2}A^{(1)}_{s-2,k}\right)>0. \tag{2.8}$$

As an example, we can choose the coefficients of the classical RK scheme for $A_{kj}^{(0)}$ and α_i, and can set

$$A_{s-2,k}^{(1)} = A_{s-1,k}^{(1)} = A_{s-2,k}^{(0)} \qquad (s = 4 \text{ and } 1 \leq k \leq s-2),$$

which satisfies (2.7) and leads to the same deterministic part in $\boldsymbol{H}_{s-2}^{(0)}$ and $\boldsymbol{H}_i^{(j)}$ $(s-2 \leq i \leq s$ and $1 \leq j \leq m)$. We will call it the SRKCL method. As another example, we can choose the coefficients of the Fehlberg 4(5) scheme [6, p. 177] for $A_{kj}^{(0)}$ and α_i, and can set

$$A_{s-2,k}^{(1)} = A_{2,k}^{(0)}, \qquad A_{s-1,k}^{(1)} = A_{3,k}^{(0)} \qquad (s = 6 \text{ and } 1 \leq k \leq s-2),$$

which satisfies (2.8) and leads to the same deterministic part in $\boldsymbol{H}_2^{(0)}$ and $\boldsymbol{H}_{s-2}^{(j)}$ or in $\boldsymbol{H}_3^{(0)}$ and $\boldsymbol{H}_i^{(j)}$ $(i = s-1, s$ and $1 \leq j \leq m)$. We will call it the SRKF45 method. Of course, the SRKCL and SRKF45 methods are of order four and five for ordinary differential equations (ODEs), respectively.

3 Mean square (MS) stability analysis

3.1 Concepts for MS stability

Before our analysis, we introduce some definitions for linear stability analysis in general form. When we substitute

$$\boldsymbol{g}_0(\boldsymbol{y}) = F\boldsymbol{y}, \qquad \boldsymbol{g}_j(\boldsymbol{y}) = G_j\boldsymbol{y} \quad (1 \leq j \leq m)$$

into (2.1), we have

$$\mathrm{d}\boldsymbol{y}(t) = F\boldsymbol{y}(t)\mathrm{d}t + \sum_{j=1}^{m} G_j\boldsymbol{y}(t)\mathrm{d}W_j(t), \qquad t > 0, \qquad \boldsymbol{y}(0) = \boldsymbol{x}_0, \tag{3.1}$$

where F and G_j $(1 \leq j \leq m)$ are real-valued square matrices of size d. This has the zero solution $\boldsymbol{y}(t) \equiv \boldsymbol{0}$ when $\boldsymbol{x}_0 = \boldsymbol{0}$ with probability one (w. p. 1). We call it the equilibrium position. Now, we can have the following concepts [1, 10].

Definition 3.1 In (3.1), the equilibrium position is said to be MS stable if, for each $\varepsilon > 0$, there exists a $\delta > 0$ such that

$$E\left[\|\boldsymbol{y}(t)\|^2\right] < \varepsilon, \quad t \geq 0$$

whenever $E\left[\|\boldsymbol{x}_0\|^2\right] < \delta$. Here, $\|\boldsymbol{y}\| \stackrel{\text{def}}{=} \left(\boldsymbol{y}^\top\boldsymbol{y}\right)^{1/2}$. Further if

$$\lim_{t\to\infty} E\left[\|\boldsymbol{y}(t)\|^2\right] = 0$$

whenever $E\left[\|\boldsymbol{x}_0\|^2\right] < \delta$, the equilibrium position is said to be asymptotically MS stable.

When we apply (2.2) to (3.1), it has the equilibrium position $\boldsymbol{y}_n \equiv \boldsymbol{0}$ with $\boldsymbol{x}_0 = \boldsymbol{0}$ (w. p. 1). Thus, we can have the following similar concepts [3,4,8,9].

Definition 3.2 Assume that a numerical method such as (2.2) is applied to (3.1) for a given $h > 0$. Then, the equilibrium position is said to be MS stable if, for each $\varepsilon > 0$, there exists a $\delta > 0$ such that

$$E\left[\|\boldsymbol{y}_n\|^2\right] < \varepsilon, \quad n \geq 0$$

whenever $E\left[\|\boldsymbol{x}_0\|^2\right] < \delta$. Further if

$$\lim_{n\to\infty} E\left[\|\boldsymbol{y}_n\|^2\right] = 0$$

whenever $E\left[\|\boldsymbol{x}_0\|^2\right] < \delta$, the equilibrium position is said to be asymptotically MS stable.

3.2 For a scalar test SDE with an m-dimensional Wiener process

In order to study stability properties, let us start with the following scalar test SDE

$$\mathrm{d}y(t) = \lambda y(t)\mathrm{d}t + \sum_{j=1}^{m} \sigma_j y(t)\mathrm{d}W_j(t), \qquad t > 0, \qquad y(0) = x_0, \tag{3.2}$$

where λ and σ_j $(1 \leq j \leq m)$ are complex values. By applying (2.2) to (3.2), we have

$$y_{n+1} = R\left(h, \lambda, \{\triangle\hat{W}_j\}_{j=1}^{m}, \{\triangle\tilde{W}_l\}_{l=1}^{m-1}, \{\sigma_j\}_{j=1}^{m}\right) y_n. \tag{3.3}$$

Here, by using $\beta_{s-1}^{(1)} = \beta_s^{(1)}$, $\beta_{s-2}^{(2)} = \sum_{i=s-2}^{s} \beta_i^{(3)} = \beta_{s-2}^{(4)} = B_{s,s-1}^{(0)} = B_{s,s-1}^{(1)} = B_{s-2,k}^{(2)} = 0$ $(s-2 \leq k \leq s)$, $\beta_{s-1}^{(2)} = -\beta_s^{(2)}$ and $\beta_{s-1}^{(4)} = -\beta_s^{(4)}$ from (2.3), we obtain

$$\begin{aligned} &R\left(h, \lambda, \{\triangle\hat{W}_j\}_{j=1}^{m}, \{\triangle\tilde{W}_l\}_{l=1}^{m-1}, \{\sigma_j\}_{j=1}^{m}\right) \\ &= c + \sum_{j=1}^{m} \triangle\hat{W}_j d_j + \sum_{j=1}^{m} \tilde{\eta}^{(j,j)}\sqrt{h}v_{jj} + \sum_{j=1}^{m}\sum_{\substack{l=1\\ l\neq j}}^{m} \tilde{\eta}^{(j,l)}\sqrt{h}v_{jl}, \end{aligned} \tag{3.4}$$

where

$$c \stackrel{\text{def}}{=} 1 + \sum_{i=1}^{s} \alpha_i h\lambda Q_{i-1}(h\lambda),$$

$$\begin{aligned} d_j \stackrel{\text{def}}{=}\ &\beta_{s-2}^{(1)}\sigma_j\hat{Q}_{s-2}(h\lambda) + 2\beta_{s-1}^{(1)}\sigma_j\hat{Q}_{s-1}(h\lambda) + \delta_1 h\lambda\sigma_j\hat{Q}_{s-2}(h\lambda) \\ &+ \alpha_s A_{s,s-1}^{(0)} B_{s-1,s-2}^{(0)} (h\lambda)^2 \sigma_j \hat{Q}_{s-2}(h\lambda), \end{aligned}$$

$$v_{jl} \stackrel{\text{def}}{=} \begin{cases} 2\beta_{s-1}^{(2)} B_{s-1,s-2}^{(1)} \sigma_j^2 \hat{Q}_{s-2}(h\lambda) & (j = l), \\ 2\beta_{s-1}^{(4)} \left(B_{s-1,s-2}^{(2)}\sigma_j\sigma_l\hat{Q}_{s-2}(h\lambda) + 2B_{s-1,s-1}^{(2)}\sigma_j\sigma_l\hat{Q}_{s-1}(h\lambda)\right) & (j \neq l), \end{cases}$$

$$\delta_1 \stackrel{\text{def}}{=} \alpha_{s-1}B_{s-1,s-2}^{(0)} + \alpha_s B_{s,s-2}^{(0)}, \quad Q_0(z) \stackrel{\text{def}}{=} 1,$$

$$Q_i(z) \stackrel{\text{def}}{=} 1 + z \sum_{k=1}^{i} A^{(0)}_{i+1,k} Q_{k-1}(z), \quad \hat{Q}_i(z) \stackrel{\text{def}}{=} 1 + z \sum_{k=1}^{i} A^{(1)}_{ik} Q_{k-1}(z) \quad (i \geq 1).$$

By noting that

$$\begin{aligned}
&E\left[\left(\tilde{\eta}^{(j,j)}\right)^2\right] = E\left[\left(\tilde{\eta}^{(j,l)}\right)^2\right] = \frac{h}{2} && (j \neq l),\\
&E\left[\tilde{\eta}^{(j,l_a)}\tilde{\eta}^{(j,l_b)}\right] = E\left[\tilde{\eta}^{(l_a,j)}\tilde{\eta}^{(l_b,j)}\right] = \frac{h}{4} && (l_a \neq l_b \text{ and } l_a, l_b > j),\\
&E\left[\tilde{\eta}^{(j,l_a)}\tilde{\eta}^{(l_b,j)}\right] = -\frac{h}{4} && (l_a \neq l_b \text{ and } l_a, l_b > j)
\end{aligned}$$

and the expectation of the other terms concerning $\tilde{\eta}^{(j,l)}$ vanishes when we take the expectation of $|R|^2$, we have

$$E\left[|R|^2\right] = |c|^2 + \sum_{j=1}^{m} h|d_j|^2 + \frac{1}{2}\sum_{j=1}^{m} h^2|v_{jj}|^2 + \frac{1}{2}\sum_{j=1}^{m}\sum_{\substack{l=1\\ l\neq j}}^{m} h^2|v_{jl}|^2. \tag{3.5}$$

Further, by substituting (2.3), (2.4) and (2.5) into this, we obtain the stability function for (2.2) as follows:

$$\begin{aligned}
&\hat{R}(p, q_1, q_2, \ldots, q_m)\\
&= \left|1 + p\sum_{i=1}^{s}\alpha_i Q_{i-1}(p)\right|^2 + \sum_{j=1}^{m} q_j \left|\frac{1}{2(B^{(1)}_{s-1,s-2})^2}\left(\hat{Q}_{s-1}(p) - \hat{Q}_{s-2}(p)\right)\right.\\
&\qquad\qquad \left. + \left(1 + \frac{1}{2}p + \frac{\alpha_s A^{(0)}_{s,s-1}(\alpha_{s-1} \pm \sqrt{\gamma_1})}{2\alpha_{s-1}(\alpha_{s-1}+\alpha_s)}p^2\right)\hat{Q}_{s-2}(p)\right|^2\\
&\quad + \frac{1}{2}\sum_{j=1}^{m} q_j^2 \left|\hat{Q}_{s-2}(p)\right|^2\\
&\quad + \frac{1}{2}\sum_{j=1}^{m}\sum_{\substack{l=1\\ l\neq j}}^{m} q_j q_l \left|\frac{B^{(2)}_{s-1,s-2}\hat{Q}_{s-2}(p) + 2B^{(2)}_{s-1,s-1}\hat{Q}_{s-1}(p)}{B^{(2)}_{s-1,s-2} + 2B^{(2)}_{s-1,s-1}}\right|^2,
\end{aligned} \tag{3.6}$$

where $\hat{R}(p, q_1, q_2, \ldots, q_m) \stackrel{\text{def}}{=} E[|R|^2]$, $p \stackrel{\text{def}}{=} h\lambda$, and $q_j \stackrel{\text{def}}{=} h|\sigma_j|^2$. The following are remarkable.

- When fourth order RK methods with four stages are embedded in our SRK methods, the first term is exactly the same in the right-hand side of (3.6) because of explicit methods [7, p. 17].
- On the other hand, when fifth order RK methods are embedded, the term in general differs, depending on each method, and their stability properties can be better than those of SRK methods in which fourth order RK methods are embedded if the noise terms are very small. However, note that the methods must satisfy the critical restriction (2.6).

Table 3.1 Butcher tableau of the SRKCL method

$\frac{1}{2}$									
0	$\frac{1}{2}$			1					
0	0	1		1	0				
$\frac{1}{2}$	0								
$\frac{1}{2}$	0	0		$B_{32}^{(1)}$					
$\frac{1}{2}$	0	0	0	$-B_{32}^{(1)}$	0				
$A_{21}^{(2)}$	$A_{22}^{(2)}$	$A_{23}^{(2)}$	$A_{24}^{(2)}$	0	0	0			
$A_{21}^{(2)}$	$A_{22}^{(2)}$	$A_{23}^{(2)}$	$A_{24}^{(2)}$	$B_{32}^{(2)}$	$B_{33}^{(2)}$	$B_{33}^{(2)}$			
$A_{21}^{(2)}$	$A_{22}^{(2)}$	$A_{23}^{(2)}$	$A_{24}^{(2)}$	$-B_{32}^{(2)}$	$-B_{33}^{(2)}$	$-B_{33}^{(2)}$			
$\frac{1}{6}$	$\frac{1}{3}$	$\frac{1}{3}$	$\frac{1}{6}$	$1-\frac{1}{2\left(B_{32}^{(1)}\right)^2}$	$\frac{1}{4\left(B_{32}^{(1)}\right)^2}$	$\frac{1}{4\left(B_{32}^{(1)}\right)^2}$	0	$\frac{1}{2B_{32}^{(1)}}$	$-\frac{1}{2B_{32}^{(1)}}$
				$-\frac{1}{2b_3^2}$	$\frac{1}{4b_3^2}$	$\frac{1}{4b_3^2}$	0	$\frac{1}{2b_3}$	$-\frac{1}{2b_3}$

Table 3.2 Butcher tableau of the SRKF45 method

$\frac{1}{4}$											
$\frac{3}{32}$	$\frac{9}{32}$										
$\frac{1932}{2197}$	$-\frac{7200}{2197}$	$\frac{7296}{2197}$									
$\frac{439}{216}$	-8	$\frac{3680}{513}$	$-\frac{845}{4104}$			$K_{F1}^{\pm}$					
$-\frac{8}{27}$	2	$-\frac{3544}{2565}$	$\frac{1859}{4104}$	$-\frac{11}{40}$		$K_{F2}^{\pm}$	0				
$\frac{1}{4}$	0	0	0								
$\frac{3}{32}$	$\frac{9}{32}$	0	0	0		$\frac{1}{2}$					
$\frac{3}{32}$	$\frac{9}{32}$	0	0	0	0	$-\frac{1}{2}$	0				
$A_{41}^{(2)}$	$A_{42}^{(2)}$	$A_{43}^{(2)}$	$A_{44}^{(2)}$	$A_{45}^{(2)}$	$A_{46}^{(2)}$	0	0	0			
$A_{41}^{(2)}$	$A_{42}^{(2)}$	$A_{43}^{(2)}$	$A_{44}^{(2)}$	$A_{45}^{(2)}$	$A_{46}^{(2)}$	$B_{54}^{(2)}$	0	0			
$A_{41}^{(2)}$	$A_{42}^{(2)}$	$A_{43}^{(2)}$	$A_{44}^{(2)}$	$A_{45}^{(2)}$	$A_{46}^{(2)}$	$-B_{54}^{(2)}$	0	0			
$\frac{16}{135}$	0	$\frac{6656}{12825}$	$\frac{28561}{56430}$	$-\frac{9}{50}$	$\frac{2}{55}$	-1	1	1	0	1	-1
						$-\frac{1}{2\left(B_{54}^{(2)}\right)^2}$	$\frac{1}{4\left(B_{54}^{(2)}\right)^2}$	$\frac{1}{4\left(B_{54}^{(2)}\right)^2}$	0	$\frac{1}{2B_{54}^{(2)}}$	$-\frac{1}{2B_{54}^{(2)}}$

- The sum of the last two terms in (3.6) is equal to $\frac{1}{2}\left(\sum_{j=1}^{m} q_j\right)^2 \left|\hat{Q}_{s-2}(p)\right|^2$ if $\hat{Q}_{s-2}(p) = \hat{Q}_{s-1}(p)$ or $B_{s-1,s-1}^{(2)} = 0$, and then $\hat{R}$ simply becomes a function of p and $\hat{q} \overset{\text{def}}{=} \sum_{j=1}^{m} q_j$. The SRKCL method satisfies the former equality.

For the SRKF45 method, let us set $B_{s-1,s-1}^{(2)}$ at 0. After all, the Butcher tableaux of the SRKCL method and the SRKF45 method are given in Tables 3.1 and 3.2. In

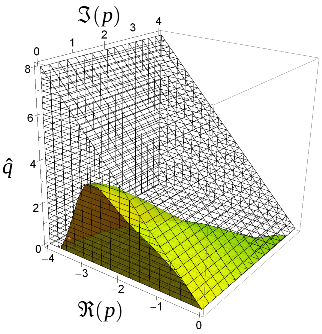

the SRKF45 method for K_{F1}^{+} and K_{F2}^{+}

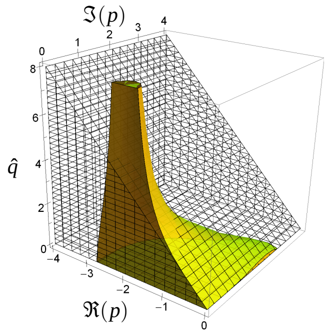

the SRKCL method

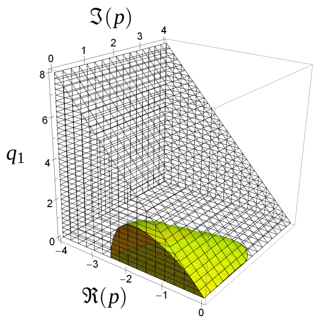

the DRI1 scheme

Fig. 3.1 MS stability domains of SRK methods

Table 3.2,

$$K_{F1}^{\pm} \overset{\text{def}}{=} \frac{5(-165 \pm 2\sqrt{1770})}{237}, \qquad K_{F2}^{\pm} \overset{\text{def}}{=} \frac{11(-50 \pm 3\sqrt{1770})}{158}$$

(double sign in same order).

If and only if $\hat{R} < 1$, the equilibrium position of (3.3) is asymptotically MS stable [8]. Let us plot the MS stability domains of our methods, that is, $\{(\Re(p), \Im(p), \hat{q}) \mid \hat{R} < 1\}$. They are given with colored parts in Fig. 3.1. The parts enclosed by mesh indicate the domain in which the equilibrium position of (3.2) is asymptotically MS stable [8]. On the other hand, because the DRI1 scheme in [5] neither satisfies $\hat{Q}_{s-2}(p) = \hat{Q}_{s-1}(p)$ nor $B^{(2)}_{s-1,s-1} = 0$, its stability function cannot be expressed with p and $\hat{q}$. For this, under the assumption $m = 1$ the MS stability domain of the scheme is given in Fig. 3.1. We can see that the SRKF45 and SRKCL methods are better than the DRI1 scheme in terms of the MS stability domain. In the figure, the following are also remarkable:

- The stability function $\hat{R}$ does not depend on $\hat{q}$ when $\Re(p) = -2$ and $\Im(p) = 0$ in the SRKCL method since $\hat{Q}_{s-1}(p) = \hat{Q}_{s-2}(p) = 1 + p/2$.
- The profile of MS stability domains for $\hat{q} = 0$ or $q_1 = 0$ shows (ordinary) stability regions for RK methods which are applied to ODEs.

3.3 For multi-dimensional non-commutative test SDEs

By applying (2.2) to (3.1), we have

$$\boldsymbol{y}_{n+1} = \boldsymbol{R}\left(h, F, \left\{\triangle\hat{W}_j\right\}_{j=1}^{m}, \left\{\triangle\tilde{W}_l\right\}_{l=1}^{m-1}, \left\{G_j\right\}_{j=1}^{m}\right)\boldsymbol{y}_n, \tag{3.7}$$

where

$$\begin{aligned}
&\boldsymbol{R}\left(h, F, \left\{\triangle\hat{W}_j\right\}_{j=1}^{m}, \left\{\triangle\tilde{W}_l\right\}_{l=1}^{m-1}, \left\{G_j\right\}_{j=1}^{m}\right)\\
&\stackrel{\text{def}}{=} C + \sum_{j=1}^{m}\triangle\hat{W}_j D_j + \sum_{j=1}^{m}\tilde{\eta}^{(j,j)}\sqrt{h}V_{jj} + \sum_{j=1}^{m}\sum_{\substack{l=1\\ l\neq j}}^{m}\tilde{\eta}^{(j,l)}\sqrt{h}V_{jl}
\end{aligned} \tag{3.8}$$

and

$$\begin{aligned}
C &\stackrel{\text{def}}{=} I + \sum_{i=1}^{s}\alpha_i hF\boldsymbol{Q}_{i-1}(hF),\\
D_j &\stackrel{\text{def}}{=} \beta_{s-2}^{(1)}G_j\hat{\boldsymbol{Q}}_{s-2}(hF) + 2\beta_{s-1}^{(1)}G_j\hat{\boldsymbol{Q}}_{s-1}(hF) + \delta_1 hFG_j\hat{Q}_{s-2}(hF)\\
&\quad + \alpha_s A_{s,s-1}^{(0)}B_{s-1,s-2}^{(0)}(hF)^2G_j\hat{Q}_{s-2}(hF),\\
V_{jl} &\stackrel{\text{def}}{=} \begin{cases} 2\beta_{s-1}^{(2)}B_{s-1,s-2}^{(1)}G_j^2\hat{\boldsymbol{Q}}_{s-2}(hF) & (j=l),\\ 2\beta_{s-1}^{(4)}\left(B_{s-1,s-2}^{(2)}G_jG_l\hat{\boldsymbol{Q}}_{s-2}(hF) + 2B_{s-1,s-1}^{(2)}G_jG_l\hat{\boldsymbol{Q}}_{s-1}(hF)\right) & (j\neq l),\end{cases}\\
\boldsymbol{Q}_0(Z) &\stackrel{\text{def}}{=} I, \quad \boldsymbol{Q}_i(Z) \stackrel{\text{def}}{=} I + Z\sum_{k=1}^{i}A_{i+1,k}^{(0)}\boldsymbol{Q}_{k-1}(Z) \quad (i\geq 1),\\
\hat{\boldsymbol{Q}}_i(Z) &\stackrel{\text{def}}{=} I + Z\sum_{k=1}^{i}A_{ik}^{(1)}\boldsymbol{Q}_{k-1}(Z) \quad (i\geq 1).
\end{aligned}$$

Here and in the sequel, I stands for the d-dimensional identity matrix. In addition, remember that δ_1 was defined in Subsection 3.2

In order to analyze stability properties of numerical methods for (3.1), Buckwar and Sickenberger [4] have introduced the MS stability matrix of numerical methods: $E[\boldsymbol{R}\otimes\boldsymbol{R}]$. Here, $\otimes$ stands for the Kronecker product. Concerning this, in a similar way to that in which we got (3.5), we obtain

$$\begin{aligned}
E\left[\boldsymbol{R}\otimes\boldsymbol{R}\right] = (C\otimes C) &+ \sum_{j=1}^{m}h\left(D_j\otimes D_j\right) + \frac{1}{2}\sum_{j=1}^{m}h^2\left(V_{jj}\otimes V_{jj}\right)\\
&+ \frac{1}{2}\sum_{j=1}^{m}\sum_{\substack{l=1\\ l\neq j}}^{m}h^2\left(V_{jl}\otimes V_{jl}\right).
\end{aligned} \tag{3.9}$$

For our SRK methods, let us seek C, D_j, V_{jj} and V_{jl} concretely. In the SRKCL method we have

$$\begin{aligned}
C &= I + hF + \frac{1}{2}(hF)^2 + \frac{1}{6}(hF)^3 + \frac{1}{24}(hF)^4,\\
D_j &= G_j + \frac{1}{2}G_j hF + \frac{1}{2}hFG_j\left(I + \frac{1}{2}hF\right)\\
&\quad + \frac{1}{6}(hF)^2 G_j\left(I + \frac{1}{2}hF\right),\\
V_{jl} &= \begin{cases} G_j^2 + \frac{1}{2}G_j^2 hF & (j = l),\\ G_jG_l + \frac{1}{2}G_jG_l hF & (j \neq l),\end{cases}
\end{aligned} \tag{3.10}$$

whereas in the SRKF45 method we have

$$\begin{aligned}
C &= I + hF + \frac{1}{2}(hF)^2 + \frac{1}{6}(hF)^3 + \frac{1}{24}(hF)^4 + \frac{1}{120}(hF)^5\\
&\quad + \frac{1}{2080}(hF)^6,\\
D_j &= G_j + \frac{1}{2}G_j hF + \frac{9}{64}G_j(hF)^2 + \frac{1}{2}hFG_j\left(I + \frac{1}{4}hF\right)\\
&\quad - \frac{1}{100}K_{F1}^{\pm}(hF)^2 G_j\left(I + \frac{1}{4}hF\right),\\
V_{jl} &= \begin{cases} G_j^2 + \frac{1}{4}G_j^2 hF & (j = l),\\ G_jG_l + \frac{1}{4}G_jG_l hF & (j \neq l).\end{cases}
\end{aligned} \tag{3.11}$$

Incidentally, in the DRI1 scheme

$$\begin{aligned}
C &= I + hF + \frac{1}{2}(hF)^2 + \frac{1}{6}(hF)^3,\\
D_j &= G_j + \frac{1}{2}G_j hF + \frac{1}{2}hFG_j + K_D(hF)^2 G_j,\\
V_{jl} &= \begin{cases} G_j^2 & (j = l),\\ G_jG_l + \frac{1}{3}G_jG_l hF & (j \neq l),\end{cases}
\end{aligned} \tag{3.12}$$

where $K_D \stackrel{\text{def}}{=} (6 - \sqrt{6})/30$.

For a non-commutative test SDE which comes from (3.1), we use

$$F = \begin{bmatrix} \lambda_1 & 0\\ 0 & \lambda_2 \end{bmatrix}, \qquad G_1 = \begin{bmatrix} \sigma_1 & 0\\ 0 & -\sigma_1 \end{bmatrix}, \qquad G_2 = \begin{bmatrix} 0 & \sigma_2\\ \sigma_2 & 0 \end{bmatrix} \tag{3.13}$$

for $d = m = 2$ and real values λ_1, λ_2, σ_1 and σ_2. This leads to a more generalized version of the test SDE that Buckwar and Sickenberger [4] have proposed.

In order to analyze stability properties of the linear d-dimensional SDE (3.1), Buckwar and Sickenberger [4] have introduced the MS stability matrix S of (3.1):

$$S \stackrel{\text{def}}{=} (I \otimes F) + (F \otimes I) + \sum_{j=1}^{m} (G_j \otimes G_j).$$

Denote by $S_{(3.13)}$ the MS stability matrix when we use (3.13). By standard calculations, we can see that the eigenvalues of $S_{(3.13)}$ are $\lambda_1 + \lambda_2 - \sigma_1^2 \pm \sigma_2^2$ and $\lambda_1 + \lambda_2 + \sigma_1^2 \pm \sqrt{(\lambda_1 - \lambda_2)^2 + \sigma_2^4}$. Thus, all eigenvalues are real values and the maximum eigenvalue is $\lambda_1 + \lambda_2 + \sigma_1^2 + \sqrt{(\lambda_1 - \lambda_2)^2 + \sigma_2^4}$. After all, if and only if

$$\lambda_1 + \lambda_2 + \sigma_1^2 + \sqrt{(\lambda_1 - \lambda_2)^2 + \sigma_2^4} < 0,$$

the equilibrium position of the test SDE is asymptotically MS stable [4]. Here, note that the inequality is rewritten as follows:

$$p_1 + p_2 + q_1 + \sqrt{(p_1 - p_2)^2 + q_2^2} < 0, \tag{3.14}$$

where $p_i \stackrel{\text{def}}{=} h\lambda_i$.

Now, let us consider the MS stability matrices of our methods when we apply them to the test SDE. The matrices can be written as a function of p_1, p_2, q_1 and q_2, say, $\hat{\boldsymbol{R}}(p_1, p_2, q_1, q_2) \stackrel{\text{def}}{=} E[\boldsymbol{R} \otimes \boldsymbol{R}]$.

From (3.9) and (3.13) as well as (3.10), (3.11) or (3.12), the eigenvalues of $\hat{\boldsymbol{R}}$ for the methods are given in the following form:

$$\begin{aligned} &v_0^{(1)} v_0^{(2)} + V_1 - q_1 v_1^{(1)} v_1^{(2)} \pm q_2 V_2, \\ &V_3^{(1)} + V_3^{(2)} \pm \sqrt{\left(V_3^{(1)} - V_3^{(2)}\right)^2 + q_2^2 V_4}, \end{aligned} \tag{3.15}$$

where the notations are defined depending on each method. For the SRKCL method,

$$\begin{aligned} &v_0^{(i)} \stackrel{\text{def}}{=} 1 + p_i + \frac{1}{2}p_i^2 + \frac{1}{6}p_i^3 + \frac{1}{24}p_i^4, \\ &v_1^{(i)} \stackrel{\text{def}}{=} \left(1 + \frac{1}{2}p_i\right)\left(1 + \frac{1}{2}p_i + \frac{1}{6}p_i^2\right), \qquad v_2^{(i)} \stackrel{\text{def}}{=} 1 + \frac{1}{2}p_i, \\ &V_1 \stackrel{\text{def}}{=} \frac{1}{2}\left(q_1^2 + q_2^2\right) v_2^{(1)} v_2^{(2)}, \qquad V_2 \stackrel{\text{def}}{=} v_1^{(1)} v_1^{(2)} - q_1 v_2^{(1)} v_2^{(2)}, \\ &V_3^{(i)} \stackrel{\text{def}}{=} \frac{1}{2}\left(v_0^{(i)}\right)^2 + \frac{1}{2}q_1\left(v_1^{(i)}\right)^2 + \frac{1}{4}\left(q_1^2 + q_2^2\right)\left(v_2^{(i)}\right)^2, \\ &V_4 \stackrel{\text{def}}{=} \prod_{i=1}^{2}\left\{\left(v_1^{(i)}\right)^2 + q_1\left(v_2^{(i)}\right)^2\right\}. \end{aligned} \tag{3.16}$$

For the SRKF45 method,

$$
\begin{aligned}
&v_0^{(i)} \stackrel{\text{def}}{=} 1+p_i+\frac{1}{2}p_i^2+\frac{1}{6}p_i^3+\frac{1}{24}p_i^4+\frac{1}{120}p_i^5+\frac{1}{2080}p_i^6\\
&v_1^{(i)} \stackrel{\text{def}}{=} 1+p_i+\left(\frac{17}{64}-\frac{K_{F1}^{\pm}}{100}\right)p_i^2-\frac{K_{F1}^{\pm}}{400}p_i^3, \qquad v_2^{(i)} \stackrel{\text{def}}{=} 1+\frac{1}{4}p_i,\\
&v_3^{(i)} \stackrel{\text{def}}{=} 1+\frac{1}{2}(p_1+p_2)+\frac{1}{8}p_1p_2+\frac{9}{64}p_i^2, \qquad v_4^{(i)} \stackrel{\text{def}}{=} 1+\frac{1}{100}p_i^2,\\
&V_1 \stackrel{\text{def}}{=} \frac{1}{2}\left(q_1^2+q_2^2\right)v_2^{(1)}v_2^{(2)},\\
&V_2 \stackrel{\text{def}}{=} \left(K_{F1}^{\pm}v_2^{(1)}v_4^{(2)}-v_3^{(1)}\right)\left(K_{F1}^{\pm}v_2^{(2)}v_4^{(1)}-v_3^{(2)}\right)-q_1v_2^{(1)}v_2^{(2)},\\
&V_3^{(i)} \stackrel{\text{def}}{=} \frac{1}{2}\left(v_0^{(i)}\right)^2+\frac{1}{2}q_1\left(v_1^{(i)}\right)^2+\frac{1}{4}\left(q_1^2+q_2^2\right)\left(v_2^{(i)}\right)^2,\\
&V_4 \stackrel{\text{def}}{=} V_2^2+q_1\left(v_1^{(1)}v_2^{(2)}+v_1^{(2)}v_2^{(1)}\right)^2.
\end{aligned}
\tag{3.17}
$$

For the DRI1 scheme,

$$
\begin{aligned}
&v_0^{(i)} \stackrel{\text{def}}{=} 1+p_i+\frac{1}{2}p_i^2+\frac{1}{6}p_i^3, \qquad v_1^{(i)} \stackrel{\text{def}}{=} 1+p_i+K_Dp_i^2,\\
&v_2^{(i)} \stackrel{\text{def}}{=} K_Dp_i^2, \qquad v_3^{(i)} \stackrel{\text{def}}{=} 1+\frac{1}{3}p_i, \qquad V_1 \stackrel{\text{def}}{=} \frac{1}{2}\left(q_1^2+q_2^2\right),\\
&V_2 \stackrel{\text{def}}{=} \left\{\frac{1}{2}\left(v_1^{(1)}+v_1^{(2)}\right)\right\}^2-\left\{\frac{1}{2}\left(v_2^{(1)}-v_2^{(2)}\right)\right\}^2-q_1v_3^{(1)}v_3^{(2)},\\
&V_3^{(i)} \stackrel{\text{def}}{=} \frac{1}{2}\left(v_0^{(i)}\right)^2+\frac{1}{2}q_1\left(v_1^{(i)}\right)^2+\frac{1}{4}\left(q_1^2+q_2^2\right),\\
&V_4 \stackrel{\text{def}}{=} \left\{\left[\frac{1}{2}\left(v_1^{(1)}+v_1^{(2)}\right)-\frac{1}{2}\left(v_2^{(1)}-v_2^{(2)}\right)\right]^2+q_1\left(v_3^{(1)}\right)^2\right\}\\
&\qquad\times\left\{\left[\frac{1}{2}\left(v_1^{(1)}+v_1^{(2)}\right)+\frac{1}{2}\left(v_2^{(1)}-v_2^{(2)}\right)\right]^2+q_1\left(v_3^{(2)}\right)^2\right\}.
\end{aligned}
\tag{3.18}
$$

We have obtained these results with the help of a symbolic computing package, *Mathematica*.

In order to plot the MS stability domains of our methods and the DRI1 scheme, let us consider the two restricted cases: $p_1 = p_2$; $q_1 = 0$. Note that each of them was considered in [4] and [20], respectively.

Case 1 ($p_1 = p_2$)

When $p_1 = p_2$, the eigenvalues of $\hat{\boldsymbol{R}}$ for the SRKCL method are

$$
\begin{aligned}
&\left(v_0^{(1)}\right)^2+\frac{1}{2}(q_1\pm q_2)^2\left(v_2^{(1)}\right)^2-(q_1\pm q_2)^2\left(v_1^{(1)}\right)^2,\\
&\left(v_0^{(1)}\right)^2+\frac{1}{2}(q_1\pm q_2)^2\left(v_2^{(1)}\right)^2+(q_1\pm q_2)^2\left(v_1^{(1)}\right)^2
\end{aligned}
$$

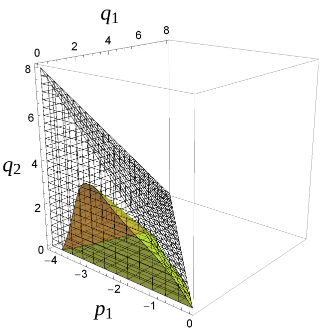

the SRKF45 method for K_{F1}^{+} and K_{F2}^{+}

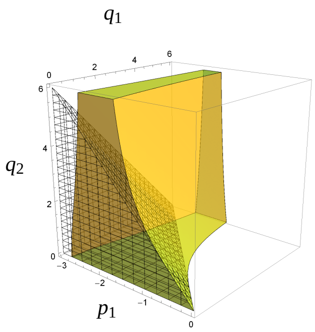

the SRKCL method

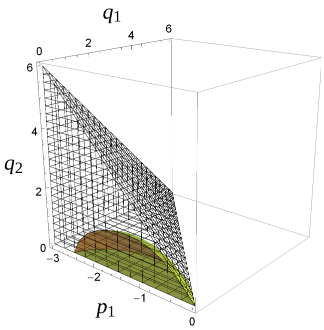

the DRI1 scheme

Fig. 3.2 MS stability domains of SRK methods when $p_1 = p_2$

(double sign in same order) from (3.15) and (3.16). Thus, the spectral radius of $\hat{\boldsymbol{R}}$, say, $\rho(\hat{\boldsymbol{R}})$ is

$$\left(v_0^{(1)}\right)^2 + \frac{1}{2}(q_1+q_2)^2\left(v_2^{(1)}\right)^2 + (q_1+q_2)\left(v_1^{(1)}\right)^2.$$

Similarly, from (3.15) and (3.17), $\rho(\hat{\boldsymbol{R}})$ is

$$\left(v_0^{(1)}\right)^2 + \frac{1}{2}(q_1+q_2)^2\left(v_2^{(1)}\right)^2 + (q_1+q_2)\left(v_1^{(1)}\right)^2$$

for the SRKF45 method, whereas from (3.15) and (3.18), $\rho(\hat{\boldsymbol{R}})$ is

$$\left(v_0^{(1)}\right)^2 + \frac{1}{2}(q_1^2+q_2^2) + (q_1+q_2)\left(v_1^{(1)}\right)^2 + q_1 q_2\left(v_3^{(1)}\right)^2$$

for the DRI1 scheme.

If and only if $\rho(\hat{\boldsymbol{R}}) < 1$, the equilibrium position of (3.7) is asymptotically MS stable [4]. Let us plot the MS stability domains of our methods and the DRI1 scheme, that is, $\{(p_1, q_1, q_2) | \rho(\hat{\boldsymbol{R}}) < 1\}$ in Case 1. They are given with colored parts in Fig. 3.2. The parts enclosed by mesh indicate the domain in which (3.14) is satisfied when $p_1 = p_2$. We can see that the SRKF45 and SRKCL methods are better than the DRI1 scheme in terms of the MS stability domain.

Case 2 ($q_1 = 0$)

When $q_1 = 0$, from (3.15) and (3.16) we obtain

$$v_0^{(1)}v_0^{(2)} + \frac{1}{2}q_2^2 v_2^{(1)}v_2^{(2)} \pm q_2 v_1^{(1)}v_1^{(2)},$$
$$V_3^{(1)} + V_3^{(2)} \pm \sqrt{\left(V_3^{(1)} - V_3^{(2)}\right)^2 + q_2^2\left(v_1^{(1)}\right)^2\left(v_1^{(2)}\right)^2}$$

as well as

$$V_3^{(i)} = \frac{1}{2}\left(v_0^{(i)}\right)^2 + \frac{1}{4}q_2^2\left(v_2^{(i)}\right)^2.$$

Now, let us denote by μ_{min} and μ_{max} the minimum eigenvalue and the maximum eigenvalue of $\hat{\boldsymbol{R}}$ for a method, respectively. Because

$$\left(V_3^{(1)} + V_3^{(2)}\right)^2 - \left\{\left(V_3^{(1)} - V_3^{(2)}\right)^2 + q_2^2\left(v_1^{(1)}\right)^2\left(v_1^{(2)}\right)^2\right\}$$
$$\geq \left\{v_0^{(1)}v_0^{(2)} + \frac{1}{2}q_2^2 v_2^{(1)}v_2^{(2)}\right\}^2 - \left(q_2 v_1^{(1)}v_1^{(2)}\right)^2,$$

thus, for the SRKCL method we obtain

$$\mu_{min} = v_0^{(1)}v_0^{(2)} + \frac{1}{2}q_2^2 v_2^{(1)}v_2^{(2)} - q_2\left|v_1^{(1)}v_1^{(2)}\right|.$$

On the other hand, for the method we can clearly see

$$\mu_{max} = V_3^{(1)} + V_3^{(2)} + \sqrt{\left(V_3^{(1)} - V_3^{(2)}\right)^2 + q_2^2\left(v_1^{(1)}\right)^2\left(v_1^{(2)}\right)^2}.$$

Similarly, from (3.15) and (3.17) we have

$$\mu_{min} = v_0^{(1)}v_0^{(2)} + \frac{1}{2}q_2^2 v_2^{(1)}v_2^{(2)} - q_2|V_2|,$$
$$\mu_{max} = V_3^{(1)} + V_3^{(2)} + \sqrt{\left(V_3^{(1)} - V_3^{(2)}\right)^2 + \left(q_2^2 V_2\right)^2},$$
$$V_2 = \left(K_{F1}^{\pm}v_2^{(1)}v_4^{(2)} - v_3^{(1)}\right)\left(K_{F1}^{\pm}v_2^{(2)}v_4^{(1)} - v_3^{(2)}\right),$$
$$V_3^{(i)} = \frac{1}{2}\left(v_0^{(i)}\right)^2 + \frac{1}{4}q_2^2\left(v_2^{(i)}\right)^2$$

for the SRKF45 method, whereas from (3.15) and (3.18) we have

$$\mu_{min} = v_0^{(1)}v_0^{(2)} + \frac{1}{2}q_2^2 - q_2|V_2|,$$
$$\mu_{max} = V_3^{(1)} + V_3^{(2)} + \sqrt{\left(V_3^{(1)} - V_3^{(2)}\right)^2 + (q_2 V_2)^2},$$
$$V_2 = \left\{\frac{1}{2}\left(v_1^{(1)} + v_1^{(2)}\right)\right\}^2 - \left\{\frac{1}{2}\left(v_2^{(1)} - v_2^{(2)}\right)\right\}^2, \qquad V_3^{(i)} = \frac{1}{2}\left(v_0^{(i)}\right)^2 + \frac{1}{4}q_2^2$$

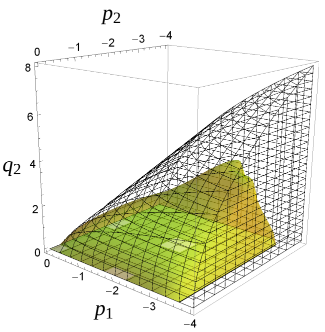

the SRKF45 method for K_{F1}^{+} and K_{F2}^{+}

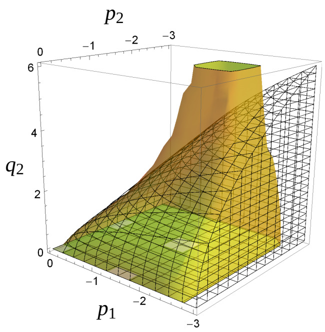

the SRKCL method

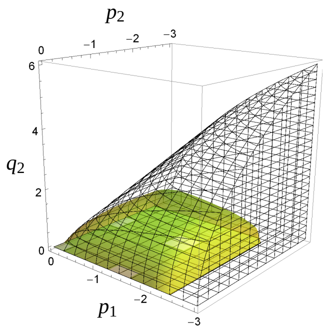

the DRI1 scheme

Fig. 3.3 MS stability domains of SRK methods when $q_1 = 0$

for the DRI1 scheme.

Noting that $\rho(\hat{\boldsymbol{R}}) = \max(|\mu_{min}|, \mu_{max})$, let us plot the MS stability domains of our methods and the DRI1 scheme, that is, $\{(p_1, p_2, q_2) \mid \rho(\hat{\boldsymbol{R}}) < 1\}$ in Case 2. They are given with colored parts in Fig. 3.3. The parts enclosed by mesh indicate the domain in which (3.14) is satisfied when $q_1 = 0$. We can see that the SRKF45 and SRKCL methods are better than the DRI1 scheme in terms of the MS stability domain.

4 Numerical experiments

In order to investigate computational efficiency and to check MS stability properties, we perform numerical experiments. Let us substitute $A_{s-2,k}^{(2)} = A_{2,k}^{(0)} \quad (1 \leq k \leq s)$ into both methods to have the same deterministic part in $\boldsymbol{H}_2^{(0)}$ and $\hat{\boldsymbol{H}}_i^{(j)}$ $(s-2 \leq i \leq s$ and $1 \leq j \leq m)$. In addition, for simplicity, we set $B_{3,2}^{(1)} = B_{3,2}^{(2)} = 1$ and $B_{3,3}^{(2)} = 0$ in the SRKCL method and $B_{5,4}^{(2)} = 1$ in the SRKF45 method. Then, we compare the numerical schemes with the DRI1 scheme in four numerical examples. As we have mentioned in Section 1, remember that the DRI1 scheme is an efficient weak second order scheme with minimized error constant.

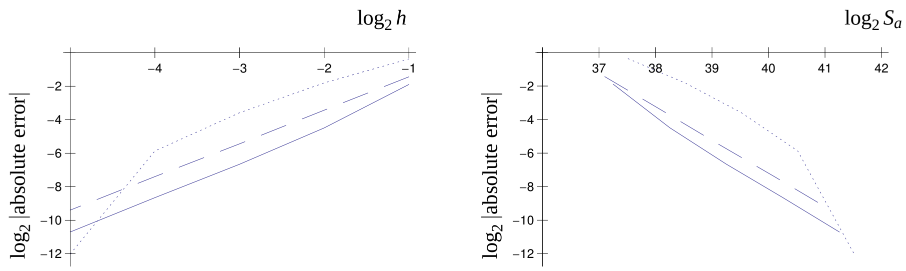

Fig. 4.1 Absolute errors about $E[f(\ln(y(t)+\sqrt{(y(t))^2+1})]$ at $t=2$. (Solid: SRKCL, dotted SRKF45, dash: DRI1.)

The first three examples come from [5]. The first example is the following non-linear SDE:

$$\mathrm{d}y(t) = \left(\frac{1}{2}y(t)+\sqrt{(y(t))^2+1}\right)\mathrm{d}t + \sqrt{(y(t))^2+1}\mathrm{d}W(t), \quad t>0, \quad y(0)=x_0.$$

Let us seek an approximation to the expectation of $f(\ln(y(t)+\sqrt{(y(t))^2+1})$ when $x_0=0$ (w. p. 1), where $f(x)\stackrel{\text{def}}{=}x^3-6x^2+8x$. The exact one is given by t^3-3t^2+2t.

In this example, using the Mersenne twister [15] we simulate 4096×10^6 independent trajectories for a given h. The results are indicated in Fig. 4.1. In the figure, the solid, dotted or dash lines denote the SRKCL, SRKF45 or DRI1 scheme, respectively. In addition, S_a stands for the sum of the number of evaluations on the drift or diffusion coefficients and the number of generated pseudo random numbers. The SRKCL scheme shows the best performance for the almost all step sizes.

The second example is the following non-commutative SDE:

$$\begin{aligned}\mathrm{d}\boldsymbol{y}(t) = &\begin{bmatrix} -\frac{273}{512} & 0 \\ -\frac{1}{160} & -\frac{785}{512}+\frac{\sqrt{2}}{8}\end{bmatrix}\boldsymbol{y}(t)\mathrm{d}t + \begin{bmatrix}\frac{1}{4} & 0 \\ 0 & \frac{1-2\sqrt{2}}{4}\end{bmatrix}\boldsymbol{y}(t)\mathrm{d}W_1(t) \\ &+ \begin{bmatrix}\frac{1}{16} & 0 \\ \frac{1}{10} & \frac{1}{16}\end{bmatrix}\boldsymbol{y}(t)\mathrm{d}W_2(t), \quad t>0, \quad \boldsymbol{y}(0)=\boldsymbol{x}_0,\end{aligned}$$

which was used in [5] to show the supremacy of the DRI1 scheme. Let us seek an approximation to the second moment of each element, $\left[E[(y_1(t))^2] \;\; E[(y_2(t))^2]\right]^\top$, when $\boldsymbol{x}_0=[1\;1]^\top$ (w. p. 1). The exact one is given by

$$\begin{bmatrix}\exp(-t) \\ \frac{149}{150}\exp(-\frac{5}{2}t)+\frac{1}{150}\exp(-t)\end{bmatrix}.$$

Here, note that if we seek $E[(y_1(t))^2]$ only, we do not need to solve the whole of the system [5].

We simulate 1024×10^6 independent trajectories for a given h. The results are indicated in Fig. 4.2. Because our present target is a vector, the Euclidean norm has been used. The SRKCL scheme shows the best performance and the SRKF45 scheme does the second best.

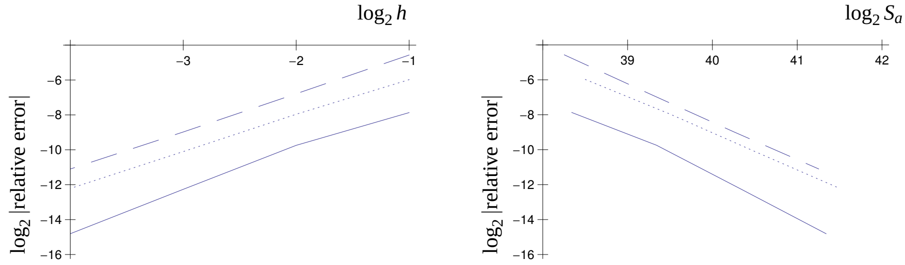

Fig. 4.2 Relative errors about the second moment at $t = 10$. (Solid: SRKCL, dotted SRKF45, dash: DRI1.)

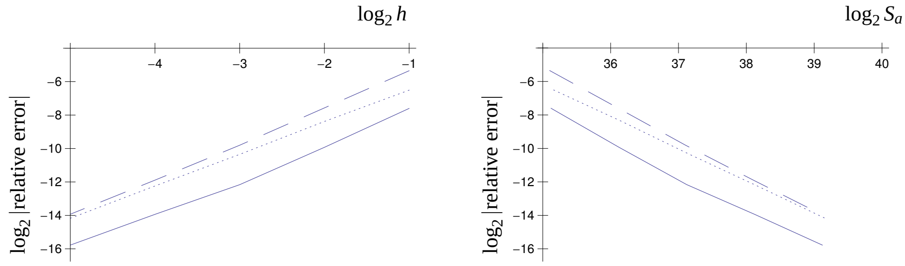

Fig. 4.3 Relative errors about the fourth moment at $t = 1$. (Solid: SRKCL, dotted SRKF45, dash: DRI1.)

The third example is the following nonlinear SDE with a 10-dimensional Wiener process:

$$\mathrm{d}y(t) = y(t)\mathrm{d}t + \sum_{j=1}^{10} \sigma_j \sqrt{y(t)+k_j}\,\mathrm{d}W_j(t), \qquad t > 0, \qquad y(0) = x_0,$$

where

$$\begin{aligned}
&\sigma_1 = \frac{1}{10}, \quad \sigma_2 = \sigma_8 = \frac{1}{15}, \quad \sigma_3 = \sigma_7 = \sigma_9 = \frac{1}{20}, \quad \sigma_4 = \sigma_6 = \sigma_{10} = \frac{1}{25}, \\
&\sigma_5 = \frac{1}{40}, \quad k_1 = k_6 = \frac{1}{2}, \quad k_2 = k_7 = \frac{1}{4}, \quad k_3 = k_8 = \frac{1}{5}, \quad k_4 = k_9 = \frac{1}{10}, \\
&k_5 = k_{10} = \frac{1}{20}.
\end{aligned}$$

This example was also used to show the supremacy of the DRI1 scheme in [5]. Let us seek an approximation to the fourth moment of its solution when $x_0 = 1$ (w. p. 1). The exact fourth moment is

$$\begin{aligned}
&(74342479604283 + 1749302625065840\exp(t) - 247988855464115218\exp(2t) \\
&\quad - 26395279310078 4216\exp(3t) \\
&\quad + 1531088033542529311\exp(4t))\,/\,\left(124416 \times 10^{13}\right)
\end{aligned}$$

(see also [13]).

We simulate 256×10^6 independent trajectories for a given h. The results are indicated in Fig. 4.3. Similarly to the results in the previous example, the SRKCL scheme shows the best performance and the SRKF45 scheme does the second best. Since this

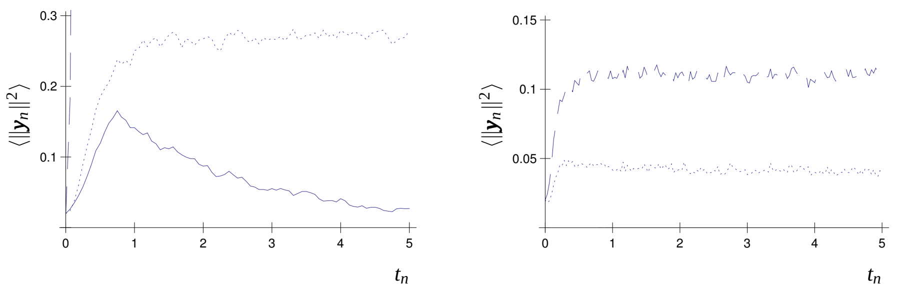

Fig. 4.4 Arithmetic means of $\|\boldsymbol{y}_n\|^2$ for $h = 1/16$ (left) and $h = 1/32$ (right). (Solid: SRKCL, dotted SRKF45, dash: DRI1.)

SDE has a 10-dimensional Wiener process, the results enhance the supremacy of the SRKCL scheme over its rivals in terms of computational costs.

The last example is the following nonlinear, non-commutative SDE:

$$\mathrm{d}\boldsymbol{y}(t) = \begin{bmatrix} \lambda & 0 \\ 0 & \lambda \end{bmatrix} \boldsymbol{y}(t)\mathrm{d}t + \sum_{j=1}^{2} \boldsymbol{g}_j(\boldsymbol{y}(t))\mathrm{d}W_j(t), \qquad t > 0, \qquad \boldsymbol{y}(0) = \boldsymbol{x}_0,$$

where

$$\boldsymbol{g}_1(\boldsymbol{y}) \stackrel{\text{def}}{=} \sigma_1 \begin{bmatrix} \frac{y_1(1-y_1)}{1+y_1^2} \\ \frac{y_2(y_2-1)}{1+y_2^2} \end{bmatrix}, \qquad \boldsymbol{g}_2(\boldsymbol{y}) \stackrel{\text{def}}{=} \sigma_2 \begin{bmatrix} \frac{y_2(1-y_1)}{1+y_1^2+y_2^2} \\ \frac{y_1(1-y_2)}{1+y_1^2+y_2^2} \end{bmatrix}.$$

Note that the linearized SDE centered at $\boldsymbol{y} = \boldsymbol{0}$ for this is equivalent to the non-commutative test SDE (3.1) with (3.13) in Case 1. Let us seek the arithmetic mean of $\|\boldsymbol{y}_n\|^2$ when $\boldsymbol{x}_0 = [0.1\ 0.1]^\top$ (w. p. 1), $\lambda = -40$ and $\sigma_1 = \sigma_2 = 6$.

We simulate 10000 independent trajectories for a given h. The results are indicated in Fig. 4.4. In the figure, $\langle \|\boldsymbol{y}_n\|^2 \rangle$ stands for the arithmetic mean of $\|\boldsymbol{y}_n\|^2$. Because the present setting satisfies (3.14), $\langle \|\boldsymbol{y}_n\|^2 \rangle$ is expected to go to 0 when t_n becomes large. For $h = 1/16$, however, only the numerical solution of the SRKCL scheme shows it and that of the DRI1 scheme explodes. On the other hand, for $h = 1/32$, $\langle \|\boldsymbol{y}_n\|^2 \rangle$ of the DRI1 scheme keeps fluctuating around 0.1 and that of the SRKF45 scheme stays around 0.05. Because the result in the SRKCL scheme is very small, we cannot see it in the figure. When $h = 1/64$, the results of these schemes numerically converge to 0.

5 Conclusions

By embedding deterministic high order RK methods into weak second order SRK methods proposed by Rößler [17], we have derived the SRKCL and SRKF45 schemes, which are of weak order two for non-commutative Itô SDEs. We have investigated their MS stability properties and shown that they have larger stability domains than those of the DRI1 scheme, which has the minimized error constant and minimal stage number for weak order two. In order to see computational efficiency and to check stability properties, we have performed numerical experiments including three examples which were used to show the supremacy of the DRI1 scheme. In all the experiments our new schemes have shown better performance than the DRI1 scheme. As a result, we have found that the embedding of the classical RK method leads to a good performance of explicit SRK methods with respect to not only stability but also computational efficiency.

Acknowledgements The authors would like to thank the referees for their valuable and careful comments which helped them to improve the earlier versions of this paper.

References

1. Arnold, L.: Stochastic Differential Equations: Theory and Applications. John Wiley & Sons, New York (1974)
2. Buckwar, E., Kelly, C.: Towards a systematic linear stability analysis of numerical methods for systems of stochastic differential equations. SIAM J. Numer. Anal. **48**(**1**), 298–321 (2010)
3. Buckwar, E., Sickenberger, T.: A comparative linear mean-square stability analysis of Maruyama and Milstein-type methods. Math. Comput. Simulation **81**(**6**), 1110–1127 (2011)
4. Buckwar, E., Sickenberger, T.: A structural analysis of mean-square stability for multi-dimensional linear stochastic differential systems. Appl. Numer. Math. **62**(**7**), 842–859 (2012)
5. Debrabant, K., Rößler, A.: Families of efficient second order Runge-Kutta methods for the weak approximation of Itô stochastic differential equations. Appl. Numer. Math. **59**, 582–594 (2009)
6. Hairer, E., Nørsett, S., Wanner, G.: Solving Ordinary Differential Equations I, Nonstiff Problems. Springer, Berlin (2000). Corrected Second Printing
7. Hairer, E., Wanner, G.: Solving Ordinary Differential Equations II, Stiff and Differential-Algebraic Systems. Springer-Verlag, Berlin (1996)
8. Higham, D.: A-stability and stochastic mean-square stability. BIT **40**(**2**), 404–409 (2000)
9. Higham, D.: Mean-square and asymptotic stability of the stochastic theta method. SIAM J. Numer. Anal. **38**(**3**), 753–769 (2000)
10. Khasminskii, R.: Stochastic Stability of Differential Equations. Springer, Berlin (2012)
11. Kloeden, P., Platen, E.: Numerical Solution of Stochastic Differential Equations. Springer, New York (1999). Corrected Third Printing
12. Komori, Y.: Weak second-order stochastic Runge-Kutta methods for non-commutative stochastic differential equations. J. Comput. Appl. Math. **206**(**1**), 158–173 (2007)
13. Komori, Y., Burrage, K.: Supplement: Efficient weak second order stochastic Runge-Kutta methods for non-commutative Stratonovich stochastic differential equations. J. Comput. Appl. Math. **235**(**17**), 5326–5329 (2011)
14. Komori, Y., Mitsui, T.: Stable ROW-type weak scheme for stochastic differential equations. Monte Carlo Methods and Appl. **1**(**4**), 279–300 (1995)
15. Matsumoto, M., Nishimura, T.: Mersenne twister: a 623-dimensionally equidistributed uniform pseudo-random number generator. ACM Transactions on Modeling and Computer Simulation (TOMACS) **8**(**1**), 3–30 (1998)
16. Rößler, A.: Second order Runge-Kutta methods for Stratonovich stochastic differential equations. BIT **47**(**3**), 657–680 (2007)
17. Rößler, A.: Second order Runge-Kutta methods for Itô stochastic differential equations. SIAM J. Numer. Anal. **47**(**3**), 1713–1738 (2009)
18. Saito, Y., Mitsui, T.: Stability analysis of numerical schemes for stochastic differential equations. SIAM J. Numer. Anal. **33**(6), 2254–2267 (1996)
19. Saito, Y., Mitsui, T.: Mean-square stability of numerical schemes for stochastic differential systems. Vietnam J. Math. **30**, 551–560 (2002)
20. Tocino, A., Senosiain, M.: Mean-square stability analysis of numerical schemes for stochastic differential systems. J. Comput. Appl. Math. **236**(**10**), 2660–2672 (2012)
21. Tocino, A., Vigo-Aguiar, J.: Weak second order conditions for stochastic Runge-Kutta methods. SIAM J. Sci. Comput. **24**(2), 507–523 (2002)